CHIN. PHYS. LETT. Vol. 38, No. 2 (2021) 026102

Pressure Driven Structural Evolutions of $0.935(Na_{0.5}Bi_{0.5})TiO_3$-$0.065BaTiO_3$ Lead-Free Ferroelectric Single Crystal through Raman Spectroscopy

Qunfei Zheng(郑群飞)[1,2,4†], Qiang Li(李强)[1,3†], Saidong Xue(薛赛东)[1], Yanhui Wu(吴延辉)[1], Lijuan Wang(王丽娟)[2], Qian Zhang(张茜)[3], Xiaomei Qin(秦晓梅)[1*], Xiangyong Zhao(赵祥永)[1], Feifei Wang(王飞飞)[1], and Wenge Yang(杨文革)[3]

[1]*Department of Physics, Mathematics & Science College, Shanghai Normal University, Shanghai 200234, China*
[2]*Center for High Pressure Science and Technology Advanced Research (HPSTAR), Beijing 100094, China*
[3]*Center for High Pressure Science and Technology Advanced Research (HPSTAR), Shanghai 201203, China*
[4]*Academy for Advanced Interdisciplinary Studies, Shenzhen Engineering Research Center for Frontier Materials Synthesis at High Pressures, Southern University of Science and Technology (SUSTech), Shenzhen 518055, China*

(Received 16 November 2020; accepted 4 December 2020; published online 27 January 2021)

Pressure evolution of local structure and vibrational dynamics of the perovskite-type relaxor ferroelectric single crystal of $0.935(Na_{0.5}Bi_{0.5})TiO_3$-$0.065BaTiO_3$ (NBT-6.5BT) is systematically investigated via *in situ* Raman spectroscopy. The pressure dependence of phonon modes up to 30 GPa reveals two characteristic pressures: one is at around 4.6 GPa which corresponds to the rhombohedral-to-tetragonal phase transition, showing that the pressure strongly suppresses the coupling between the off-centered A- and B-site cations; the other structural transition involving the oxygen octahedral tilt and vibration occurs at pressure ∼13–15 GPa with certain degree of order-disorder transition, evidenced by the abnormal changes of intensity and FWHM in Raman spectrum.

DOI: 10.1088/0256-307X/38/2/026102

Lead based piezoelectric solid solutions have been widely used in sensors, actuators and energy harvesting devices because of their superior ferroelectric and piezoelectric properties.[1] As the fast development of modern society and the high demands of bio- and environmental-friendly functional materials, lead-free piezoelectric systems with high-performance have gradually become a research hotspot.[2,3] Among these compounds, $Na_{1/2}Bi_{1/2}TiO_3$ (NBT) based ceramics merit as one of excellent candidates for high performance lead-free piezoelectric materials. NBT is a perovskite (ABO_3) ferroelectric in which two different cations, Na^+ and Bi^{3+} at A site, can fit in the lattice simultaneously.[4–6] $(1-x)(Na_{1/2}Bi_{1/2}TiO_3)$-$x BaTiO_3$ (NBT-100xBT) solid solution is one of the most common binary lead-free ferroelectric systems, which contains multiple coexisting phases (e.g., $R3c$, $P4bm$ and $P4mm$) as a function of x.[7] It has been reported that there is a morphotropic phase boundary (MPB) near x values of 0.05–0.07 in the NBT-100xBT binary system, and the piezoelectric coefficient can reach up to 420 pC/N, which is completely comparable to the most widely used commercial lead-based $Pb[Zr_xTi_{1-x}]O_3$(PZT).[7–11] Previous work showed that NBT-100xBT has the highest piezoelectric constants and electric field induced strains near the MPB region,[10] which needs to be further explored or tuned to find possible mechanism underlying for better material design.

The general method to map phase evolutions and the corresponding desired properties of the ferroelectric materials is mainly through chemical doping or temperature-dependent behavior. Pressure is also the basic thermodynamic parameter to study the structure phase transitions and physical properties of ferroelectric materials. The nondestructive Raman scattering is a powerful technique for investigating phase transition in NBT-based solid solutions,[12–15] and is also an ideal method for diamond anvil cell (DAC) high pressure experiment. In fact, most of the reports have discussed the Raman features that are temperature-dependent. Rout *et al.*[16] reported the spectral changes for the NBT-100xBT system at room temperature, whereas Datta *et al.*[15] and Huang *et al.*[12] worked on different temperatures. The *in situ* high pressure x-ray scattering and Raman spectroscopic results on relaxor ferroelectric NBT has been reported,[17–19] and it was concluded that there ap-

Supported by the National Natural Science Foundation of China (Grant Nos. 11674231, 11974250, and 51772192), the Science and Technology Commission of Shanghai Municipality (Grant Nos. 17070502700 and 19070502800), and the Shenzhen Development and Reform Commission Foundation for Shenzhen Engineering Research Center for Frontier Materials Synthesis at High Pressures.

†Qunfei Zheng and Qiang Li contributed equally to this work.
*Corresponding author. Email: xmqin@shnu.edu.cn
© 2021 Chinese Physical Society and IOP Publishing Ltd

pears to be rhombohedral-to-orthorhombic crystal-structural transitions ($R3c$ to $Pnma$) at 3.3 GPa. Kreisel *et al.*[19] reported the Raman spectra to show octahedral tilt mode from $a^-a^-a^-$ to $a^-b^+a^-$, A-cation displacement from parallel $[111]_p$ to antiparallel $[100]_p$, B-cation restore to the center of symmetry, therefore the displacement from $[111]_p$ to $[000]_p$.[20,21] In addition, $ZnTiO_3$ and $BaTiO_3$ also have pressure-induced structural transitions.[22,23]

In this Letter, we report the pressure-driven structural transformations in NBT-xBT single crystals studied by *in situ* Raman spectroscopy over a pressure range from ambient pressure to 30 GPa. The aim of our study is to determine structural transition and local lattice dynamics through quantitative analysis of spectra. At 4.6 GPa and ∼13–15 GPa, the Raman spectrum changes significantly, which indicates the appearance of a high-pressure phase. By analyzing the Raman shift, relative intensity and full width at half maximum (FWHM), it is concluded that the A- and B-site off-center displacement of NBT-6.5BT under high pressure is suppressed, and the tilt and vibration of oxygen octahedron is enhanced.

The NBT-6.5BT single crystal sample was grown by the top-seeded solution growth (TSSG) method,[24] the crystals were oriented along the [001] direction using an x-ray diffractometer. The Ba^{2+} doping ratio is determined by x-ray fluorescence spectroscopy, and the ambient pressure phase structure is confirmed using x-ray diffraction, and more detailed information can be found in Ref. [25].

In-situ high pressure Raman experiments at room temperature were conducted in a symmetric DAC with diamond culet size of 300 μm in diameter. A small piece (∼60 μm × 60 μm × 10 μm) of NBT-6.5BT single crystal was loaded into a sample chamber of 100 μm in diameter drilled in the center of a T301 stainless-steel gasket (pre indented to a thickness of ∼30 μm). Silicone oil was used as the pressure-transmitting medium and the applied pressure was determined by the ruby fluorescence method.[26] The Raman experiment was performed in a Renishaw inVia Raman microscope equipped with a 2400 grooves/mm grating and a spectral resolution of around 2 cm^{-1}. The excitation source was an argon ion laser (532 nm) focused down to a size of 10 μm in diameter. The spectra are fitted with Gauss–Lorenz peak-shape functions.

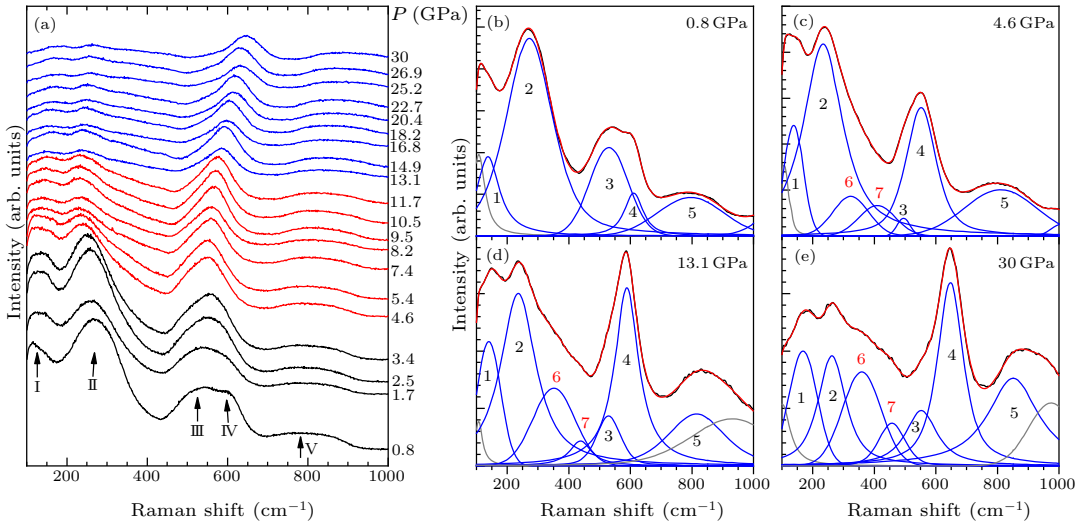

Fig. 1. (a) Pressure-dependent Raman spectra for $(Na_{0.5}Bi_{0.5})TiO_3$-6.5$BaTiO_3$ single crystal from 0.8 GPa to 30 GPa. The shifts and splitting of the phonon bands are due to structural phase transitions with increasing pressure. (b)–(e) Raman spectra (black solid lines) for $(Na_{0.5}Bi_{0.5})TiO_3$-6.5$BaTiO_3$ single crystals at 0.8 GPa, 4.6 GPa, 13.1 GPa and 30 GPa, respectively. The resultant spectrum profiles (red solid lines) fitting by the Gauss–Lorentz function. The blue thin lines mark the Raman peaks for which the pressure evolution is further discussed.

The ideal perovskite structure is cubic with space group ($Pm\bar{3}m$) and therefore there are no Raman-active modes. However, there are Raman modes in many perovskite-type ferroelectric materials,[19,27] which are related to the deformation of the structure, e.g., A-site cations deviate from the symmetric center, or B-site cations deviate from the center of the oxygen octahedron, or the tilt and vibration of the octahedron itself. As mentioned earlier, NBT-100xBT samples have rhombohedral symmetry with space group $R3c$ and tetragonal symmetry with space group $P4bm$ at different compositions. Based on the factor-group analysis, $R3c$ phase has 13 Raman active modes: $\Gamma_{\text{Raman}} = 7A_1 + 6E$, while $P4bm$ has 15 Raman active modes: $\Gamma_{\text{Raman}} = 3A_1 + 3B_1 + 2B_2 + 7E$.[19,21]

Figure 1(a) shows the overall evolution of the Raman spectra of NBT-6.5BT from ambient pressure to 30 GPa. The Raman spectra has undergone important pressure-induced changes, which can be described by changes in band characteristics and the appear-

ance of new spectral features. It can be seen that all major peaks are relatively broad due to the A-site disorder.[14,28] At relatively low pressure, the Raman spectrum is divided into four main frequency bands. For the convenience, the modes are hereafter identified as I, Ⅱ, (Ⅲ, Ⅳ) and V as denoted in Fig. 1(a). In the low-wavenumber region, band I ($\sim$140 cm^{-1}) is associated to the A-BO_3 translation mode involving vibrations of both A- and B-site cations, therefore it is sensitive to coupling processes between off-centered A-site and B-site cations.[14] Band Ⅱ is located at about 200–350 cm^{-1} and is related to the vibrations of B-site cations that are sensitive to B-cation off centering (200–300 cm^{-1} corresponding to A_1 symmetry, 300–350 cm^{-1} to B_1 symmetry).[21,29,30] In high-wavenumber region (labeled as Ⅲ and Ⅳ), the band of $\sim$400 cm^{-1} is from the BO_6 tilting mode, which can also be considered as A–O bond stretching. The mode between 450 and 650 cm^{-1} is contributed to the oxygen octahedral vibrations.[21,31] Finally, the weak band V (above 700 cm^{-1}) is very likely to be the A_1 (longitudinal optical) and E (longitudinal optical) overlapping bands.[29] The vibrations related to the A and B cations in NBT-xBT are dominated by ferroelectrically active Bi^{3+} and Ti^{4+}, respectively.[15] To quantitatively evaluate the four main frequency bands, we have fitted the spectrum profiles with Gauss–Lorentz function. In the representative curves shown in Figs. 1(b)–1(e), the NBT-6.5BT Raman spectrum at 0.8 GPa can be deconvoluted into four peaks in the range of 100–700 cm^{-1}, but it can be deconvoluted into six peaks from 4.6 GPa to 30 GPa. As shown in Fig. 1, the obvious difference between the low- and high-pressure Raman spectra indicates that the structural rearrangement with applied pressure. The Raman active modes for the ambient coexisting phases ($R3c$ and $P4bm$) can be clearly identified. According to Raman spectra [Fig. 1(b)] at 0.8 GPa, it can be seen that there is no peak of the B_1 mode, indicating the existing of $R3c$ phase; and the doublet splitting of phonon modes appears in the high wavenumber region, showing a feature of tetragonal phase.[30,32,33] This is consistent with the NBT-100xBT system having MPB character at $x = 0.06$–0.07, where a rhombohedral $R3c$ and a tetragonal $P4bm$ symmetry coexist.[34] At 4.6 GPa [Fig. 1(c)], the B_1 (peak 6) mode, a main feature of tetragonal phase structure, appears with weak signal. At the same time, the appearance of peak 7 indicates a complete transition from the ambient coexisting phases to the tetragonal phase. According to the study of Ma *et al.*,[8] the space group of the NBT-100xBT tetragonal phases can be either $P4bm$ or $P4mm$, so we suggest that the change of the Raman spectrum of 4.6 GPa corresponds to the transition from the $R3c/P4bm$ coexisting phase to the $P4bm/P4mm$ coexistence phase. At 13.1 GPa [Fig. 1(d)], Raman spectroscopy does not show any additional phonon modes. Through the above discussion, we believe that structural transition takes place near 4.6 GPa. Furthermore, the intensity evolution and band shift of Raman spectra can also be used to identify phase transition in classic and complex ferroelectrics.[23,24] In order to identify all the possible structural changes, the peak positions, the FWHMs and the integral intensities of peaks in the Raman spectra are plotted in Figs. 2–4.

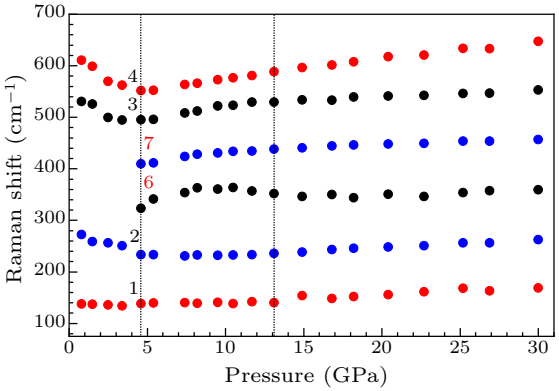

Fig. 2. The band frequency as a function of pressure in the Raman spectra for $(Na_{0.5}Bi_{0.5})TiO_3$-6.5$BaTiO_3$ single crystal.

Figure 2 shows the evolution of the frequency positions of all the observed Raman peaks versus pressure. The mode at 130 cm^{-1} (peak 1) exhibits no significant pressure shift from ambient pressure up to 13.1 GPa, compared with other peaks, suggesting that strength of coupling processing between off-centered Bi^{3+} and off-centered Ti^{4+} cations is less modulated by external pressure.[15] The vibrational band moves to a higher frequency with further increasing pressure. The prominent change is that the peaks 2, 3, and 4 show red shift from ambient pressure up to 4.6 GPa. In the Raman spectra of $BaTiO_3$ and $PbTiO_3$, a similar signature is observed in the middle-frequency region (300–350 cm^{-1}). This negative frequency shift has been interpreted to a soft-mode behavior described as a pressure-induced phase transition. In addition, two new modes begin to appear at 323 cm^{-1} (peak 6) and 410 cm^{-1} (peak 7) when pressure is higher than 4.6 GPa. The frequency of B_1 (peak 6) mode displays high-wavenumber shifts first and then low-wavenumber shifts in the range of 4.6–13.1 GPa, and it is nearly insensitive to pressure when the pressure is higher than 13.1 GPa. Previous studies have shown that discontinuous change of mode frequencies, disappearance of mode and the emergence of new mode are typical characteristics of a phase transition in a perovskite ferroelectric.[19,22,23] Through above-mentioned abnormal changes in Raman spectra, we propose that the structural transition takes place at 4.6 GPa.

The change of phonon modes can be explained not only by the frequency of Raman spectra, but also by the intensity and FWHM of Raman spectra. According to previous reports, the excess FWHM can be analyzed by hard-mode Raman spectroscopy.[35] Such studies have been reported on the relaxor ferroelectric, pressure-induced evolution of FWHM and intensity of phonon modes to provide deeper insight into intrinsic structural peculiarities.[15,19,36] Figure 3 shows the intensity and FWHM of the phonon modes at ∼130 cm^{-1} [Figs. 3(a) and 3(b)] and in the range of 200–350 cm^{-1} [Figs. 3(c) and 3(d)]. As can be seen in Fig. 3, there are significant differences among the three modes in the pressure range studied. The peak 1 (the dominant mode is ω_1) is related to the A-BO_3 translation mode, involving vibrations of both A-site Bi^{3+} and B-site Ti^{4+}, and it is expected to be sensitive to phase transition. However, Pb-based relaxors indicate that this Raman scattering mirror can be explained by the coupling processes between off-centered A- and B-site cations.[37,38] From the perspective of the overall intensity change in Fig. 3(c), ω_1 intensity shows insignificant changes. However, the FWHM clearly increases with increasing pressure in Fig. 3(a), showing that the pressure causes strong coupling between the off-centered A- and B-site cations. In addition, previous studies of relaxors have shown that the increase of the FWHM and the intensity of the lowest-energy mode near the phase transition are due to the coupling with the flip mode.[39] The phonon mode located at 200–350 cm^{-1} is Ti-O vibration, which is related to the off-center displacement of Ti^{4+} cations. At 4.6 GPa, the B_1 (peak 6) mode appears, whose dominant mode is ω_6, suggesting that the structure becomes a tetragonal phase. The ω_2 mode (peak 2) has larger FWHM and intensity than ω_6 mode (peak 6) in the low-pressure range. On the other hand, the FWHMs of ω_2 mode and ω_6 mode have a dramatic discontinuous change taking place at ∼ 13–15 GPa. The FWHM and peak intensity are important for studying the off-center displacement of B-site cations.[40] At relatively low pressure, the FWHM and intensity of ω_2 do not change much, indicating that low pressure has relatively less effect on B-site cations. When the pressure exceeds 4.6 GPa, the intensity of ω_2 rapidly decreases, indicating that the pressure suppresses the off-center displacement of the B-site cations. The abnormal changes of the intensity and FWHM of Raman modes,[36] indicate an order-disorder entangled phase transition occurring in the pressure range of 13–15 GPa. The previous discussion suggested that the phase transformation from the $R3c/P4bm$ coexisting phase to the $P4bm/P4mm$ coexistence phase at 4.6 GPa. For the $P4bm$ and $P4mm$ phases, the Raman spectra are indistinguishable. However, the first principles calculation shows that when compressing the lattice volume, the free energy of $P4bm$ is lower than that of $P4mm$, so $P4bm$ is more stable under higher pressure compared to $P4mm$.[7] We believe that the change of the Raman spectrum at ∼ 13–15 GPa corresponds to the transition from the $P4bm/P4mm$ coexistence phase to the $P4bm$ single phase. Above 15 GPa, the intensity of ω_2 decreases linearly in dependence on pressure. On the other hand, the decrease of FWHM also indicates the long-range order of the B-site cations increasing. The off-center displacement of A- and B-site cations is the nature of spontaneous polarization in displacive ferroelectric materials. Due to the high pressure suppress the off-center displacement of A- and B-sites cations, the spontaneous polarization of NBT-6.5BT is expectedly reduced under high pressure.

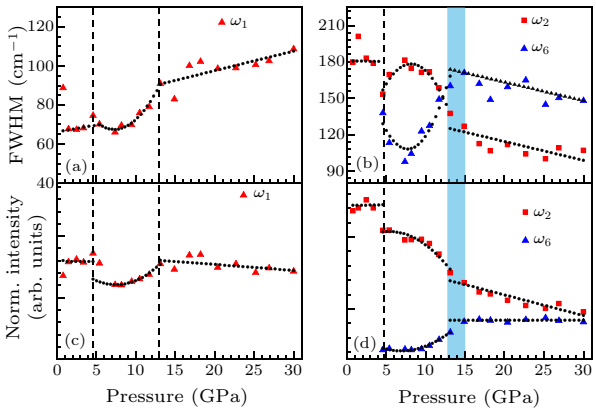

Fig. 3. Pressure evolution of the FWHM (a) and (b), and the intensity of the Na-localized mode (c) and Ti-localized mode (d) in $(Na_{0.5}Bi_{0.5})TiO_3$-6.5$BaTiO_3$ single crystal. Black dashed lines indicate the phase transition points, the gray dotted lines are guides for the eyes.

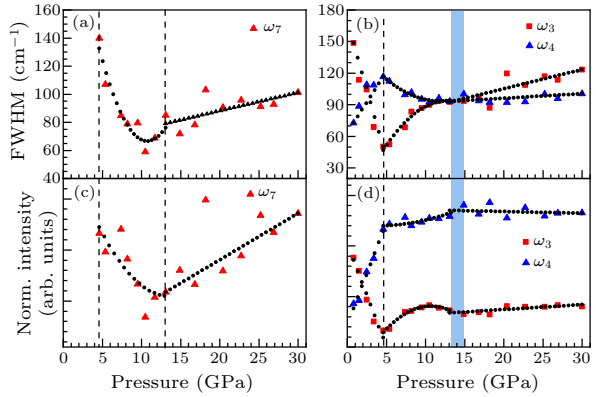

Fig. 4. Pressure evolution of the FWHM and intensity of the oxygen octahedron tilting mode [(a), (b)] and oxygen octahedron vibration mode [(c), (d)] in $(Na_{0.5}Bi_{0.5})TiO_3$-6.5$BaTiO_3$ single crystal. Black dashed lines indicate the phase transition points, the gray dotted lines are guides for the eyes.

Figures 4(a)–4(d) show the FWHM and intensity of the phonon modes of oxygen octahedral tilting (ω_7) and vibration (ω_3, ω_4) versus pressure. The effect of Ba doping is mainly from the destruction of long range

due to the large radius of Ba^{2+} ions,[41,42] promoting the off-center displacement of A- and B-site cations and suppressing the tilt of oxygen octahedron.[42] Therefore, when the pressure is lower than 4.6 GPa, there is no octahedral tilted phonon mode appearing. Previous studies of Pb-based perovskite-type relaxor ferroelectrics demonstrated that high pressure favors BO_6 tilting.[43] At 4.6 GPa, the ω_7 phonon mode (near 400 cm^{-1}) appears, which is related to TiO_6 tilts, indicating that $P4bm$ and $P4mm$ coexist. The intensity turns to increase at around 13.1 GPa, at which $P4mm$ fully transforms to $P4bm$. According to the previous study of Jones and Thomas, the oxygen octahedron tilting pattern of $P4bm$ is $(a^0a^0c^+)$, and the displacements of B-site cations (Ti^{4+}) are antiparallel to those of A-site cations (Bi^{3+}, Na^+, and Ba^{2+}) along the polar [001] direction.[44] Above 15 GPa, the intensity increases linearly with pressure, because the oxygen octahedral tilt facilitates the $P4bm$ phase by forming a more compact structure.[7] The phonon mode of the high wavenumber is related to the vibration of the oxygen octahedron. FWHM values of the modes ω_3 and ω_4 below 4.6 GPa exhibit decreasing and increasing trends, respectively. According to the neutron diffraction experiment, the R-type octahedral rotations superlattice peak appears in the rhombohedral phase, which occurs at the $q = (111)\pi/a$ point of the Brillouin zone, and the M-type superlattice peak appears in the tetragonal phase, which occurs at the $q = (111)\pi/a$ point of the Brillouin zone.[45] In the Raman spectra, a triplet splitting of the oxygen octahedral vibration modes in the rhombohedral phase, and a doublet splitting in tetragonal phase.[33] In our experiments, the overall frequency band is doublet splitting, but the FWHM of ω_3 is very large at lower pressure, indicating that the ambient-condition phase does include rhombohedral phase. Support comes from the fact that the signature of the high-pressure Raman spectrum of NBT-6.5BT is very similar to those observed in the high-pressure phase of pure NBT single crystals.[19] As a result, the band does not change visibly above 4.6 GPa.

Pressure also has a great influence on structural and ferroelectric properties of perovskite ferroelectrics.[19,46–49] In order to improve our understanding of the pressure-induced changes in the dielectric properties of relaxor ferroelectrics, more detailed studies on the influence of pressure in relaxor ferroelectrics are needed. In the future work, we will carry out pressure-dependent ferroelectric hysteresis loop and dielectric spectroscopy measurements, to deeply understand the ferroelectric and dielectric properties of the occurring phase transitions.

In conclusion, the pressure-induced NBT-6.5BT single crystal Raman spectral change is obvious, the pressure contributes to the oxygen octahedral tilt and causes strong coupling between the off-centered A- and B-site cations. The evolution of Raman spectrum under pressure indicates that there are two structural transitions. The first phase transition occurring near 4.6 GPa corresponds to the transition from the $R3c/P4bm$ to the $P4bm/P4mm$ coexisting phase. A pure $P4bm$ phase can be obtained with further increasing pressure to above 15 GPa. Further x-ray studies, which can give detailed crystal structure of the high-pressure phase, are needed to clarify the conclusions.

We thank Dr. Jinlong Zhu for helpful discussion.

References

[1] Jaffe B, Cook W R and Jaffe H 1971 *Piezoelectric Ceramics* (London: Academic Press)
[2] Saito Y, Takao H, Tani T, Nonoyama T, Takatori K, Homma T, Nagaya T and Nakamura M 2004 *Nature* **432** 84
[3] Rodel J, Jo W, Seifert K T P, Anton E M, Granzow T and D 2009 *J. Am. Ceram. Soc.* **92** 1153
[4] Li Y, Chen W, Zhou J, Xu Q, Sun H and Liao M 2005 *Ceram. Int.* **31** 139
[5] Li Y, Chen W, Xu Q, Zhou J, Gu X and Fang S 2005 *Mater. Chem. Phys.* **94** 328
[6] Takenaka T, Maruyama K and Sakata K 1991 *Jpn. J. Appl. Phys.* **30** 2236
[7] Ma C, Guo H Z, Beckman S P and Tan X L 2012 *Phys. Rev. Lett.* **109** 107602
[8] Li F, Zhang S J, Xu Z and Chen L Q 2017 *Adv. Funct. Mater.* **27** 1700310
[9] Kang S J L, Park J H, Ko S Y and Lee H Y 2015 *J. Am. Ceram. Soc.* **98** 347
[10] Chiang Y M, Farrey G W and Soukhojak A N 1998 *Appl. Phys. Lett.* **73** 3683
[11] Jin C F, Zhang S Q, Shen Z Q and Li W L 2019 *Chin. Phys. Lett.* **36** 107701
[12] Eerd B W, Damjanovic D, Klein N, Setter N and Trodahl J 2010 *Phys. Rev. B* **82** 104112
[13] Huang T, Guo S, Xu L P, Chen C, Luo H S, Chu J H and Hu Z G 2015 *J. Appl. Phys.* **117** 224103
[14] Kreisel J and Glazer A M 2000 *J. Phys.: Condens. Matter* **12** 9689
[15] Datta K, Richter A, Göbbels M, Neder R B and Mihailova B 2014 *Phys. Rev. B* **90** 064112
[16] Rout D, Moon K S, Rao V S and Kang S J L 2009 *J. Ceram. Soc. Jpn* **117** 797
[17] Kreisel J, Bouvier P, Dkhil B, Thomas P A, Glazer A, Welberry T, Chaabane B and Mezouar M 2003 *Phys. Rev. B* **68** 014113
[18] Thomas P A, Kreisel J, Glazer A M, Bouvier P, Jiang Q and Smith R 2005 *Z. Kristallogr.* **220** 717
[19] Kreisel J, Glazer A, Bouvier P and Lucazeau G 2001 *Phys. Rev. B* **63** 174106
[20] Glazer A M 1972 *Acta Crystallogr. Sect. B: Struct. Crystallogr. Cryst. Chem.* **28** 3384
[21] Kreisel J, Glazer A M, Jones G, Thomas P A, Abello L and Lucazeau G 2000 *J. Phys.: Condens. Matter* **12** 3267
[22] Ruiz-Fuertes J, Winkler B, Bernert T, Bayarjargal L, Morgenroth W, Koch-Müller M, Refson K, Milman V and Tamura N 2015 *Phys. Rev. B* **91** 214110
[23] Venkateswaran U D, Naik V M and Naik R 1998 *Phys. Rev. B* **58** 14256
[24] Zhang H W, Chen C, Deng H, Ren B, Zhao X Y, Lin D, Li X B and Luo H S 2014 *J. Mater. Chem. C* **2** 10124

[25] Zheng Q, Zhao X, Sun R and Luo H 2011 *Phys. Status Solidi A* **208** 1012
[26] Mao H K, Bell P M, Shaner J W and Steinberg D J 1978 *J. Appl. Phys.* **49** 3276
[27] Zhang M S and Scott J F 1986 *Ferroelectr. Lett. Sect.* **6** 147
[28] Trujillo S, Kreisel J, Jiang Q, Smith J H, Thomas P A, Bouvier P and Weiss F 2005 *J. Phys.: Condens. Matter* **17** 6587
[29] Wang J, Zhou Z and Xue J 2006 *Acta Mater.* **54** 1691
[30] Deluca M, Picht G, Hoffmann M J, Rechtenbach A, Töpfer J, Schader F H and Webber K G 2015 *J. Appl. Phys.* **117** 134110
[31] Schütz D, Deluca M, Krauss W, Feteira A, Jackson T and Reichmann K 2012 *Adv. Funct. Mater.* **22** 2285
[32] Cordero F, Craciun F, Trequattrini F, Mercadelli E and Galassi C 2010 *Phys. Rev. B* **81** 144124
[33] Luo L, Ge J, Li J, Viehland D, Farley C, Bondnar R, Zheng Q and Luo H 2011 *J. Appl. Phys.* **109** 113507
[34] Rout D, Moon K S, Park J and Kang S J L 2013 *Curr. Appl. Phys.* **13** 1988
[35] Bismayer U 1990 *Phase Transit.* **27** 211
[36] Welsch A M, Mihailova B, Gospodinov M, Stosch R, Güttler B and Bismayer U 2009 *J. Phys.: Condens. Matter* **21** 235901
[37] Welsch A M, Maier B J, Mihailova B, Angel R J, Zhao J, Paulmann C, Engel J M, Gospodinov M, Marinova V and Bismayer U 2011 *Z. Kristallogr.* **226** 126
[38] Waeselmann N, Mihailova B, Maier B J, Paulmann C, Gospodinov M, Marinova V and Bismayer U 2011 *Phys. Rev. B* **83** 214104
[39] Salje E, Devarajan V, Bismayer U and Guimaraes D M C 1983 *J. Phys. C* **16** 5233
[40] de la F G, Malcherek T, Gorfman S and Mihailova B 2017 *Phys. Rev. B* **96** 214102
[41] Hill N A and Rabe K M 1999 *Phys. Rev. B* **59** 8759
[42] Baettig P, Schelle C F, LeSar R, Waghmare U V and Spaldin N A 2005 *Chem. Mater.* **17** 1376
[43] Maier B J, Angel R J, Marshall W G, Mihailova B, Paulmann C, Engel J M, Gospodinov M, Welsch A M, Petrova D and Bismayer U 2010 *Acta Crystallogr. Sect. B: Struct. Crystallogr. Cryst. Chem.* **66** 280
[44] Jones G O and Thomas P A 2002 *Acta Crystallogr. Sect. B: Struct. Crystallogr. Cryst. Chem.* **58** 168
[45] Fujii Y, Hoshino S, Yamada Y and Shirane G 1974 *Phys. Rev. B* **9** 4549
[46] Zhu J L, Jin C Q, Cao W W and Wang X H 2008 *Appl. Phys. Lett.* **92** 242901
[47] Han W, Zhu J L, Zhang S J, Zhang H, Wang X H, Wang Q L, Gao C X and Jin C Q 2013 *J. Appl. Phys.* **113** 193513
[48] Zhu J L, Xiao C J, Chi Z H, Feng S M, Li F Y, Jin C Q, Deng X Y, Wang X H, Li L T, Dai Z H, W J and Xu Z 2006 *Chin. Phys. Lett.* **23** 1631
[49] Li F Y, Jin C Q, You S J, Xiao C J, Yu R C, Wang X H, Liu J, Li X D, Li Y C and Chen C L 2006 *Chin. Phys. Lett.* **23** 1249